The Cryosphere Discuss., 6, 4517–4555, 2012
www.the-cryosphere-discuss.net/6/4517/2012/
doi:10.5194/tcd-6-4517-2012

The Cryosphere Discussions

Scenario-based climate change modelling for a regional permafrost probability model of the southern Yukon and northern British Columbia, Canada

P. P. Bonnaventure[1,2] **and A. G. Lewkowicz**[2]

[1]Department of Geography, Queen's University, Kingston, Canada
[2]Department of Geography, University of Ottawa, Ottawa, Canada

Received: 12 September 2012 – Accepted: 15 September 2012 – Published: 24 October 2012

Correspondence to: P. P. Bonnaventure (philip.bonnaventure@queensu.ca)

Published by Copernicus Publications on behalf of the European Geosciences Union.

Abstract

Scenario-based climate change modelling for equilibrium conditions was applied to a Regional Model of permafrost probability for the southern Yukon and northwestern British Columbia. Under a −1 K cooling scenario, permafrost area expands from 58 % (present day) of the 490 000 km^2 to 76 %, whereas warming scenarios of +1 K, +2 K and +5 K decrease the terrain underlain by permafrost to 38 %, 24 % and 9 % respectively. The morphology of permafrost gain/loss under these scenarios is controlled by the Surface Lapse Rate (SLR), which varies across the region below and above treeline. The SLR is an air temperature elevation gradient that that is noticeably different across the study region. As a result of this attribute three distinct patterns of loss morphology can be identified. Areas that are more maritime exhibit SLRs characteristically similar above and below treeline resulting in low probabilities of permafrost in valley bottoms. Consequently, a loss front moves to upper elevations when warming scenarios are applied (Simple Unidirectional Spatial Loss). Areas where SLRs are gentle below treeline (but normal/negative) and normal above treeline show lower permafrost probabilities with a loss front moving up mountain according to two separate SLRs (Complex Unidirectional Spatial Loss). Finally areas that display high continentally exhibit Bidirectional Spatial Loss where the loss front of lower permafrost probabilities moves up mountain above treeline and down mountain below treeline. Areas that are most affected by permafrost loss are zones with SLRs close to 0 K km^{-1} where permafrost is extensive, whereas the least susceptible areas to changes in MAAT are above treeline and are highly elevation dependent.

1 Introduction

Anthropogenically-induced climate change is expected to be heightened in arctic and subarctic areas (IPCC, 2007; ACIA, 2005) and its effects on the cryosphere are predicted to be particularly important (ACIA, 2005). Impacts on permafrost, defined as

TCD
6, 4517–4555, 2012

earth materials which remain at a temperature of 0 °C or below for two or more consecutive years (ACGR, 1988; French, 2007; Williams and Smith, 1989), are less well-defined than effects on sea ice and glaciers, in part due to incomplete or inadequate baseline information. However, as permafrost is the only element of the cryosphere that is inhabited by people year-round, it is essential to understand the ramifications and the potential risks associated with permafrost in a changing climate. Permafrost distribution at the regional scale is strongly related to climate through the Mean Annual Air Temperature (MAAT). However, the presence of mountain permafrost in the discontinuous zone relates to a series of complex factors (Shur and Jorgensen, 2007; Gruber and Haeberli, 2009), including elevation, depth of snow cover, slope, aspect, geology and vegetation (Lewkowicz and Ednie, 2004; Lewkowicz and Bonnaventure, 2008; Bonnaventure and Lewkowicz, 2008, Gruber and Haeberli, 2009). As the polar amplification of climate change continues to progress, terrain within the discontinuous permafrost zone (10–50 % permafrost coverage) where permafrost is warm and most sensitive, is likely to undergo considerable change (Romanovsky et al., 2010; Smith et al., 2010).

The discontinuous permafrost zone of the Western Cordillera of North America represents a zone of significant economic and strategic importance for the resource industry in Canada. This area includes communities with year round populations, roads and resource infrastructure projects. The range of effects of climate change on permafrost include warming of surface and temperatures at depth (IPCC, 2007; ACIA, 2005), increasing active layer thickness (Haeberli et al., 1993; Burn and Zhang, 2010; SWIPA, 2012; Bonnaventure and Lamoureux, 2012), basal melt resulting in permafrost thinning (Harris et al., 2001; Woo et al., 2008), precipitation and hydrological changes (Woo et al., 2008), the development of thermokarst features (Harris et al., 2001; Woo et al., 2008) as well as natural hazards associated with permafrost degradation (Kääb, 2008). Climate change will likely affect permafrost slopes, possibly generating or enhancing mass movements such as creep-related processes, rockslides, rock falls, mudslides, and active layer detachment failures (Evans & Clague, 1994; Harris et al., 2001;

TCD
6, 4517–4555, 2012

Lewkowicz and Harris, 2005; Dorren, 2003; Lipovsky et al., 2006; Haeberli et al., 2006; Kääb, 2008).

The goal of this paper is to examine the changes to permafrost extent predicted for the southern half of the Yukon and extreme northern British Columbia (Bonnaventure et al., 2012), when Mean Annual Air Temperature (MAAT) shifts of −1 K to +5 K are applied. This scenario-based modelling reveals the spatial pattern of permafrost loss and permits a classification of the pattern of potential permafrost degradation, highlighting how this changes across the study region.

2 Study region

The study region covers between 59° N to 65° N and from 141° W to as far east as 123°5′ W representing approximately 490 000 km^2 (Fig. 1). This region is considered to be part of the Cordilleran orogen geological grouping, comprising large mountain belts of deformed and metamorphosed sedimentary and volcanic rocks, mainly of the Phanerozoic and Proterozoic ages (DEMR, 1974; Wahl et al., 1987; Eyles and Miall, 2007). During the Wisconsinan glacial maximum, the southern and central portions of the study area were covered by the thick ice masses of the Cordilleran ice sheet whereas the northwestern portion around the Dawson area was unglaciated (Duk-Rodkin, 1996).

Elevations range from 250 m a.s.l. in the Yukon River valley to greater than 5000 m a.s.l. in the St. Elias Mountains. The region encompasses all terrestrial permafrost zones, from isolated patches in the southwest to continuous in the most northerly areas (Heginbottom et al., 1995). The entire region is in the Boreal Cordillera ecozone, which is characterized by mountain ranges with many lofty peaks and extensive plateaus with long, cold winters and short, warm summers, varying with elevation and mountainside orientation (Natural Resources Canada, 2010).

Climatic gradients across the region are relatively gentle except in the southwest where there is a strong precipitation gradient from 1415 mm at Pleasant Camp to

TCD
6, 4517–4555, 2012

270 mm at Whitehorse over a distance of 150 km. Continentality increases northward and eastward. Annual precipitation (outside the St. Elias) ranges between about 300 and 400 mm with the highest amounts in the Liard Basin climatic region (Wahl et al., 1987). The entire study region experiences winter-time inversions in surface lapse rates (SLR) through the forested zone (Lewkowicz and Bonnaventure, 2011). The results of inverted SLRs on an annual basis are increased permafrost probabilities in valley bottoms in areas of high continentality while in more maritime environments, SLRs are gentle but normal, so that permafrost is less common at low elevations and in parts of northern British Columbia there is a lower elevational limit (Lewkowicz et al., 2012). The changes in SLR at treeline have been observed throughout the study region over multiple years but the reasons for these changes remain unclear and require farther study (Lewkowicz and Bonnaventure, 2011).

Vegetation in the region comprises boreal forest with coniferous trees and some boreal broadleaf trees in lowland areas, while sub-alpine forest, shrubs, alpine tundra, barren patches, and exposed rock occur progressively at higher elevations (Wahl et al., 1987; Kremer et al., 2011). The northernmost portion of the study area is very close to an ecosystem boundary where vegetation begins to transition to arctic tundra with alpine sedges, grasses and shrubs dominating (Wahl et al., 1987).

Climatic regions in relation to the individual study areas are shown in Figure 1 and are described more fully in previous publications (Lewkowicz and Ednie, 2004; Lewkowicz and Bonnaventure, 2008; Bonnaventure and Lewkowicz, 2012). The area itself also contains over 20 communities with a combined population of greater than 25 000 permanent inhabitants.

TCD
6, 4517–4555, 2012

3 Methods

3.1 Regional permafrost model creation

The Regional Permafrost Model (Bonnaventure et al., 2012) is an empirical-statistical model, which relates field data collected in both winter and summer to variables calculated from a Digital Elevation Model (DEM) in a Geographic Information System (GIS) environment. The model's main input is more than 2000 Basal Temperature of Snow (BTS) and ground truthing data points collected in seven intense study sites within the region (2001–2009) (Fig. 1). BTS measurements provide point indications of permafrost likelihood that can be related statistically to factors such as elevation, equivalent elevation (e.g. Lewkowicz and Bonnaventure, 2011) slope, and Potential Incoming Solar Radiation (PISR). BTS measurements are calibrated using checks of the physical presence of permafrost in the late summer, allowing permafrost probability to be calculated across a spatial surface using logistic regression (e.g. Lewkowicz and Ednie, 2004). Individual permafrost probability models were created for areas ranging from 200–1500 km^2 (Fig. 1). Interpolation between intense study locations was undertaken using a blended distance decay function (Bonnaventure et al., 2012).

A novel aspect of the Regional Model is the use of equivalent elevation as the primary DEM derived variable. The relationship between permafrost distribution and elevation in this area is complex and valley bottoms are also at relatively high elevations (typically 300–700 m a.s.l.) where permafrost may be present. The concept of equivalent elevation (Lewkowicz and Bonnaventure, 2011) was developed to deal with these complexities. Actual elevations in a DEM are adjusted to reflect mean annual air temperatures based on local Surface lapse Rates (SLR). The numerical elevations of grid cells below treeline are changed to take into account weakened or reversed SLRs in the forest compared to the strong normal negative SLRs above treeline. Thus grid cells that are well below treeline may be increased significantly in elevation, areas close to treeline are changed very little and areas above treeline remain unchanged. Equivalent

TCD
6, 4517–4555, 2012

elevation is evaluated numerically from:

$$Z'_x = Z_t - (Z_t - Z_x) \times \frac{L_1}{L_2} \quad (1)$$

where Z'_x is equivalent elevation (m a.s.l.), Z_t is the elevation of treeline (m a.s.l.), Z_x is actual grid cell elevation (m a.s.l.), L_1 is the measured or predicted SLR below treeline ($^\circ C\,km^{-1}$) and L_2 is the SLR above treeline (assumed to be $-6.5\,^\circ C\,km^{-1}$). The derivation of equivalent elevation surface for the entire study is described completely in Lewkowicz and Bonnaventure (2011).

The Regional Model shows that under current conditions 58 % of the study region is underlain by permafrost across several geographically distinct areas (Fig. 3) (Bonnaventure et al., 2012). The Regional Model has also been independently validated using the modeled results for the Sa Dena Hes area, a model created within the study region but not used in the regional model (Bonnaventure and Lewkowicz, 2012), the boundaries compared to the national permafrost map of Canada (Heginbottom et al., 1995), a database of Yukon rock glaciers (Page, 2009) as well as a series of instrumented boreholes (Global Terrestrial Network for Permafrost, 2011).

3.2 Regional Model perturbation for climate change scenarios

A range of warming values including +1 K, +2 K and +5 K were investigated based on IPCC and ACIA predictions for the upcoming century. Scenario temperature changes in this paper are indicated in degrees Kelvin (K) rather than degrees Celsius ($^\circ C$) in order to indicate change and avoid confusion with MAATs which are recorded in Celsius. This approach was favored rather than using Global or Regional Climate Model predictions due to the problem of adequately representing the topography in the Western Cordillera (see Burn, 1994). In addition permafrost conditions have also been investigated under a cooler climate (−1 K), which may have existed during the Little Ice Age (Farnell et al., 2004). This choice of −1 K air temperature was selected because dendrochronological results for the region show that maximum temperatures during summers from

TCD
6, 4517–4555, 2012

1684–1850 AD were generally 0–1 K colder than in the 1961–1990 reference period (Youngblut and Luckman, 2008) but summer temperatures may exhibit less variability than annual values. Consequently, it must be emphasize that we are exploring the impacts of scenarios of past cooling and potential future warming in this paper, rather than indicating that such changes took place or will take place.

Changes in MAAT were simulated in the spatial model by uniformly increasing the value of the equivalent elevations variable in the transformed DEM for cooling scenarios and decreasing them for warming scenarios (Janke, 2005; Bonnaventure and Lewkowicz, 2010) and then running the model to produce an altered BTS surface. This in turn affects the predicted permafrost probabilities that are calibrated with the non-linear logistic regression coefficients determined for the base (present-day) case. An equivalent elevation change of 154 m represents 1 K of change. The equivalent elevation surface effectively standardizes the different SLR values around the study region so that a uniform scenario change is distinctively responded to in a given area. As an example in highly maritime environments such as Haines Summit SLR below treeline is virtually equivalent to the standard environmental lapse rate of $-6.5\,\mathrm{K\,km^{-1}}$, whereas in areas such as Johnson's Crossing the SLR is much gentler ($-2.4\,\mathrm{K\,km^{-1}}$) or inverted in highly continental areas such as Dawson ($+0.7\,\mathrm{K\,km^{-1}}$). The equivalent elevation equation takes into account the SLR differences when the transformation is performed, so that a uniform change is perceived differently in distinct portions of the region based on geography. This method has the benefit of preserving all elements of the spatial model for a given area such as aspect, shading and slope, as well as the specific relationships that exist between changes in BTS values and elevation.

4 Results

The impact of changing the MAAT through the scenario approach shows different affects on the distribution of permafrost based on the geographic region, controlled by the unique SLR of the specific area. Thus as a consequence the results of the MAAT

TCD
6, 4517–4555, 2012

scenarios can be examined to show overall changes to permafrost distribution as well as on a more zonal level. Overall throughout the region the change in permafrost distribution thru the different scenarios follows roughly an exponential decay curve (Fig. 2). Under current conditions (base case) 58 % of the unglaciated territory is underlain by permafrost according to the Regional Model (Bonnaventure et al., 2012). Examining the −1 K cooling scenario (Fig. 4) for the region, the amount of area underlain by permafrost expands by 18 % to cover a total of 76 % of the currently unglaciated territory. It is likely that during a period where MAATs was one degree colder than present glacial territory would also expand, however, this relationship is not examined in this paper and as a result all scenarios do not consider glacial change in extent calculations. Investigating the warming scenarios, a +1 K change (Fig. 5) decreased the area underlain by permafrost to 38 %. Here a +1 K change decreases the area underlain by permafrost by 20 % making the initial degree of warming the most significant with respect to the overall amount of permafrost lost (Fig. 9). A +2 K change (Fig. 6) farther reduces the area to 24 % underlain, whereas a warming of +5 K (Fig. 7) shows widespread permafrost loss with only 9 % remaining.

Seeing as the study region is very large ($\approx 490\,000\,km^2$) in order to see how the climate change scenarios affect the distribution of permafrost, the Regional Model has to be split up into zones based on geographic similarities. The Regional Model was broken down into geographic areas, which included an extreme southwest portion, as well as south, mid and north zones (Fig. 8). These geographic areas also coincide with areas of similar SLRs and as a result show similar behavior with respect to permafrost spatial change patterns when the scenarios are applied. When the results are examined according to the region break (Fig. 8) it shows that the gain/loss of permafrost differs. The overall amount of permafrost as well as the change curve in each of the zones is seen in Fig. 9. The pattern of overall change in each of the zones shows the most abrupt change is seen in the RM +1 K model and in the northern zone. In addition the northern zone shows the maximum overall area underlain by permafrost of the four zones in each of the scenarios except for the +5 K warming where the overall area dips

TCD
6, 4517–4555, 2012

below that of the Mid zone (10.8 % in the North, 11.6 in the Mid at +5 K). This implies that this zone is more susceptible to both short- and long-term changes in MAAT.

Examining the gain/loss patterns according to a distribution of pixels in bands of permafrost probability (0.1 probability bands) allows for an examination of how the probabilities are being altered in each zone (Fig. 10). In the extreme southwest (ESW) the pattern of gain/loss is highly predictable and the curve is simply shifted vertically representing the percent of area underlain by permafrost however, remaining with relatively the same shape throughout all the scenarios. The ESW contains a very high numbers of cells in the lower probabilities (< 0.2), very few cells through the remainder of the probabilities and then shows a secondary peak in probabilities above 0.8 in all scenarios except +5 K. In the South region the pattern is similar to that seen in the ESW however, there is a peak in the number of pixels between 0.1 and 0.2. This peak essentially remains in the same place throughout the different scenarios but increases in magnitude as warming is amplified. There is again a secondary increase in the number of cells in the upper probabilities however, this increase is less abrupt in the South and occurs over a much larger range of probabilities. In the Mid region there is a clear peak in which probabilities are most represented in each scenario. As warming is simulated the peak shifts toward lower probabilities (e.g. RM −1 K = 0.8–0.9, RM = 0.6–0.7, RM +1 K = 0.3–0.4, RM +2 K = 0.1–0.2, RM +5 K = 0–0.1). In the North region the majority of cells in both the base case and the −1 K scenario are between 0.8–0.9. As warming is applied the curve of probabilities is flattened with a more even distribution of probabilities before shifting toward a peak of the lowest probabilities (0–0.1) at the +5 K scenario.

5 Discussion

The idea of perturbing permafrost models in mountain areas in order to explore the distribution change has been examined using similar input variable changes for smaller areas (Janke, 2005; Bonnaventure and Lewkowicz, 2010). These models have been

TCD
6, 4517–4555, 2012

highly elevation based, and thus show significant changes with warming as lower permafrost probabilities move up mountain to higher elevations when warming scenarios are applied. This application of the models is correct in areas above treeline where the use of fixed SLRs is appropriate (e.g. Bonnaventure and Lewkowicz, 2010). Over the area of the Yukon and British Columbia where the Regional Model predicts, this method is not accurate, as expanding modeled results to areas below treeline is necessary (Lewkowicz and Bonnaventure, 2011). The Regional Model is the only empirical statistical model to be derived using the outlined empirical statistical techniques for such a large area while keeping a resolution of 30 × 30 m. In addition it is also the first model to incorporate the effect of variable SLRs across a region of complex topography. The perturbation of the Regional Model is unique as it shows non-linear elevation based permafrost changes, as the coldest areas are not necessarily reflected by the highest elevations. Thus the perturbation of this model allows for an understanding of permafrost loss morphology, which is particularly important at the community and linear infrastructure route-planning level. How the landscape will evolve with respect to permafrost in a warming climate provides awareness into what areas are susceptible to small changes (1–2 K warming, short-term) as well as larger changes (2–5 K warming, long-term).

The behavior of the distribution of permafrost in each of the regional zones (Figs. 11–13) is essentially the product of the climate, which is generalized through the value of the SLR. More maritime locations have SLRs that are very similar to normal ($-6.5\,\mathrm{K\,km^{-1}}$) whereas the most continental locations show higher tendencies toward inverted (positive) SLRs (Lewkowicz and Bonnaventure, 2011). In order to comprehend how susceptible an area is to potential permafrost loss an understanding of the potential loss morphology in each region must be analyzed. Because each region has a distinct range of SRL values, this will control the relative amount of the area that is exposed to potential permafrost gain/loss. Areas that have SLRs close to $0\,\mathrm{K\,km^{-1}}$ (no temperature change with elevation) are essentially elevation independent, whereas those that have SLR that approach normal ($-6.5\,\mathrm{K\,km^{-1}}$) can be viewed as elevation

TCD
6, 4517–4555, 2012

dependent. This means that in elevation independent areas, such as those in and approaching the North region, a +1 K scenario change will affect area across much greater elevation band.

5.1 Loss morphology types

Understanding how permafrost distribution will change as climate warms is perhaps the most important attribute for planning at the community level as it provides knowledge into the time scale of susceptibility. Examining the morphology of the loss, effectively three different types of loss patterns can be identified (Table 1). The first type is termed Simple Unidirectional Spatial Loss (SUSL) (Figs. 11 and 14) this type of loss would occur in areas that have a normal SRLs ($-6.5\,\mathrm{K\,km^{-1}}$) both above and below treeline. These environments are located in the ESW region and in the Regional Model, have very low probabilities of permafrost (0–0.1) in valley bottoms and up to treeline. Above treeline, permafrost probabilities begin to increase with elevation and approach or reach continuous (>0.9) at the highest elevation locations. As a result of only one SLR both below and above treeline, when a warming scenario is applied the lowest probabilities, which are in the valley bottoms progressively move to higher elevations. The movement of lower probabilities in a given direction with elevation can be termed the loss front. In an area of SUSL the loss pattern behaves similar to that seen in previous models, which are highly elevation dependent (e.g. Bonnaventure and Lewkowicz, 2010) and would generally react this way if applied to other empirical-statistical model for areas such as the European Alps (e.g. Gruber and Hoelzle, 2001). In the Regional Model, areas that display SUSL, include the study area of Haines Summit as well as the majority of the ESW where the largest areas of glaciers, the tallest mountains and the most precipitation in the region is seen annually (Fig. 14). This also however, represents the area with the smallest population and least amount of infrastructure for the region itself.

A similar but more complicated loss pattern is termed Complex Unidirectional Spatial Loss (CUSL) (Figs. 12 and 14). This loss pattern is seen in areas that have

TCD
6, 4517–4555, 2012

normal (negative) SLRs throughout the area however; below treeline the SLR is gentle (e.g. $-2.5\,K\,km^{-1}$) compared to a strong normal SLR above treeline ($-6.5\,K\,km^{-1}$). As a result when a warming scenario is applied the loss front moves up the elevation bands both above and below treeline but according to two separate rates relative to its position. Essentially this means that in the area above treeline, where the majority of the permafrost is located the area is more elevation dependent than the area below treeline. Thus assuming permafrost was ubiquitous across a mountain (complete coverage) above and below treeline, the area below treeline would lose permafrost over a larger elevation band compared to above treeline given the same warming scenario. As a result, the area above treeline is more resistant to small changes in MAAT (e.g. +1 K). This area in the region contains the study areas of Wolf Creek, Ruby Range, Johnson's Crossing, Sa Dena Hes and Faro. Also of note is that the area susceptible to CUSL includes the largest population centers in the region including Whitehorse the Territorial capital of the Yukon (population > 22 000).

The final form of spatial loss pattern is the most complex, as the loss front moves in two distinct directions; this pattern is termed Bidirectional Spatial Loss (BSL) (Figs. 13 and 14). In order for this pattern to be observed the SLR in an area through the forest must be inverted (positive). In the area of the Regional Model this occurs in the most continental areas of the North region, here SLRs are observed or modeled between ranges 0 to $+1\,K\,km^{-1}$. In areas of BSL the highest probabilities of permafrost are located in both the mountaintops above treeline and in the valley bottoms below treeline where cold air is able to pool (Clements et al., 2003; Pagès and Miró, 2009; Lewkowicz and Bonnaventure, 2011). As a warming scenario is simulated the loss front moves up the mountain from treeline toward the mountain peak above treeline, whereas below treeline the loss front moves from treeline down toward the valley bottom. The area below treeline however, has a SLR much closer to $0\,K\,km^{-1}$ which makes the area elevation independent, losing permafrost over a larger elevation range below treeline than above for the same level of MAAT change. This makes the areas that are subject to BSL below treeline, very susceptible to small MAAT scenario changes. According to

TCD
6, 4517–4555, 2012

the modelling, given any amount of MAAT warming these areas would be affected the most and loose significant amounts of permafrost most rapidly. Located within the area prone to BSL includes the study areas of Keno and Dawson (also the second largest population center in the region), as well as Beaver Creek, a town located on an Alaska Highway border crossing.

From examining the different types of spatial loss, areas that are most susceptible to potential permafrost loss appear to be sectors that have SLRs at or very close to $0\,K\,km^{-1}$. These areas are elevation independent below treeline meaning that when a scenario change is applied all area across elevation bands below treeline are prone to permafrost loss and essentially there is no loss front. Susceptibility to small changes can thus be characterized according to which areas are most prone to short-term changes, where areas that are most elevation independent have the highest susceptibility to changes in MAAT (Fig. 15). Areas with SLRs that are closest to normal ($-6.5\,K\,km^{-1}$) as well as all areas above treeline are thus most elevation dependent and will have distinct loss fronts. From examining Fig. 15, one attribute that can be noticed is that the areas that are most susceptible are located in areas that currently have generally high probabilities of permafrost. This is significant in the context of climate change in the area of the Regional Model as it means significant change will occur in areas with substantial permafrost probabilities. In addition when changes occur in environments where permafrost is central to the geomorphic and ecosystem functions of the system both above and below treeline, significant environmental shifts can occur. This environmental geoclimatic shifts include the results of transitioning from an environment with permafrost to one without including increased likelihoods of natural hazards including landslides and surface hydrological changes (Kneisel et al., 2007; Kääb, 2008). Changes to the landscape evolution through the vegetation (Jorgensson et al., 2001) as well as potential changes to carbon cycling of the environment and the potential release of stored greenhouse gases in permafrost are also a potential consequence (Tarnocai et al., 2009; Hugelius et al., 2010; O'donnell et al., 2011).

TCD
6, 4517–4555, 2012

5.2 Model limitations

It is important to note that the models presented here, as well as the patterns of loss morphology are essentially conceptual. These models examine potential changes to the distribution of permafrost under equilibrium conditions. As a result they do not take into account transient effects or lag times. It is well understood that permafrost at depth is subject to considerable lag times when climate or surface conditions change including snow cover (e.g. Burn and Nelson 2006; Lawrence et al., 2008). In addition areas of ice-rich permafrost or areas that have well-developed transition layers (e.g. Shur et al., 2005) are considerably resilient to small changes in MAAT (Froese et al., 2008), which is not accounted for. Although much of the study region can be considered mountain permafrost, which normally contains lower ground ice content, as well as considerable exposed bedrock, which reacts relatively quickly to changes in MAAT, lags can still exist. A considerable source of both lag and uncertainty in this environment is due to the high contains of thick organic mats especially in the forested and lower elevational tundra zones. These organic controls can act to environmentally sustain cold temperatures in the ground even under short sustained periods of MAAT $> 0\,^{\circ}$C (Williams and Smith, 1989; Shur and Jorgensson, 2007). As a result this can considerably increase lag times so long as the organic content is not subject to removal by mechanisms including forest fire or road construction (Shur and Jorgensson, 2007).

Another possible drawback to this scenario-based modelling of potential permafrost change is seen in the type of scenario change that is implemented in the warming scenario itself. The MAAT scenario change implies uniform warming throughout the different seasons, which is not necessarily what is predicted under current GCMs (IPCC, 2007; SWIPA, 2012). Although it is generally accepted that warming is occurring throughout the Polar Regions, and at a greater rate than other portions of the world the amount of change is not predicted to be uniform throughout the seasons (ACIA, 2005; IPCC, 2007; SWIPA, 2012). Many predictions show that the majority of warming is likely to occur in the winter and autumn seasons (IPCC, 2007; CAS, 2010). Although changes

TCD
6, 4517–4555, 2012

are not as pronounced in the summer or thawing season, recent studies have shown that winter warming can have significant impacts on permafrost degradation and thickening of the active layer as freeze-back is delayed in the fall (Burn and Zhang, 2010). The primary concern however, about this differential warming is that this could potentially disrupt the patterns of SLRs throughout the region. The SLR is controlled by the range of temperatures between mean January and mean July air temperature. Higher air temperature ranges (i.e. higher continental environments) yield greater likelihoods of inversions below treeline, whereas lower ranges result in more maritime climates with normal SLRs below treeline (Lewkowicz and Bonnaventure, 2011). This is significant because the more pronounced the winter warming is in the region the greater the range of temperatures will decrease. The decrease means that the pattern of temperature trends with elevation is likely to change as long-term climate establishes a new balance. As a result of this, the areas that are likely to be most effected with respect to understanding the loss morphology occur in the areas of the North which are prone to BSL as well as the areas which show SLRs at or close to $0\,K\,km^{-1}$. These changes however, are likely only to change the patterns significantly in the more aggressive of the warming scenarios (e.g. +5 K) as this is the only scenario where significant change to climate has already occurred and it is presumed would take relatively significant time to occur ($\geq$ 2100 AD) (IPCC, 2007). It is also important to note that although the patterns could be changed due to differential change in seasonal warming thus altering the SLR patterns, the conceptual loss morphology types (SUSL, CUSL and BSL) would still apply. It is however, important to note that the proportions and spatial distribution of permafrost in each are likely somewhat subject to change. In order to examine this region for the effects of variable SLR change and how this would impact the permafrost distribution, statistical downscaled GCM data would be needed and a new equivalent elevation surface would have to be calculated factoring in the changed SLRs. Because however, these models represent equilibrium permafrost conditions it is also important to understand that a secondary lag would also exist between changes in MAAT as well as the establishment of new SLRs in each of the areas of the region. Thus at

TCD
6, 4517–4555, 2012

present the outlined models are the most likely scenario in the short-term, when permafrost is subject to initial thaw. This topic outlines one of the key limitations of the current presented methodology for determining permafrost distribution changes using the Regional Model and should be considered in future study.

6 Conclusions

The following conclusions can be reached as a result of this research:

1. From examining the different scenarios of permafrost gain/loss in the area of the Regional Model the extent of permafrost coverage, which is currently modeled at 58 %, changes along a roughly exponential curve. Predicted permafrost extents vary from 76 % under a −1 K cooling to 9 % when a +5 K warming is applied including +1 K (38 %) and +2 K (24 %).

2. The amount and pattern of permafrost change is different for distinctive areas in the Regional Model. Areas in the ESW portion show elevation dependent SUSL which moves along one loss front up mountain. Patterns of CUSL are seen in the majority of the South and Mid regions where different loss fronts move up mountain above and below treeline but according to different degrees of elevation dependence. In the most continental North region, where SLRs are inverted BSL is observed, here change moves along a descending loss front below treeline, and along an ascending loss front above treeline.

3. The areas most susceptible to short-term permafrost loss include the areas where SLRs are very close to 0 K km^{-1}. These areas are found below treeline in the North regions of the model which are elevation independent meaning that when a change in MAAT is applied the scenario effects permafrost over the greatest range of elevations. The areas that are least susceptible to potential permafrost change include areas above treeline where SLRs are normal (−6.5 K km^{-1}) and elevation dependent.

TCD
6, 4517–4555, 2012

4. The use of these models in understanding the patterns of potential permafrost loss are of direct use to climate adaptations strategies as well as resource and linear infrastructure-route planning in the region. The modelling has effectively outlined the potential patterns of change in permafrost distribution in this area of complex topography, which is a key factor in determining hazards associated with permafrost degradation.

5. The application of this type of empirical-statistical permafrost modelling to examine the effects of equilibrium climate change on permafrost can be applied to similar models including those for the European Alps. Modelling is driven through the primary altered variable of equivalent elevation and any modelling must include local knowledge of SLRs to properly understand how permafrost distribution changes with elevation.

6. A major limitation of this modelling is that these models examine potential changes to the distribution of permafrost under equilibrium conditions; as a result they do not take into account transient effects or lag times. In addition the warming/cooling scenarios applied assume uniform change through the seasons which is not predicted with current GCMs. The potential drawback of non-uniform warming is that this can change the patterns of SLRs within the area, which is linked to the range of seasonal air temperatures.

Acknowledgements. This project was supported financially by the Canadian Foundation for Climate and Atmospheric Sciences, the Federal Government of Canada's International Polar Year Program, the Natural Sciences and Engineering Research Council of Canada, the Northern Scientific Training Program (Department of Indian Affairs and Northern Development), the Yukon Geological Survey, the Geological Survey of Canada, and the Faculty of Arts, University of Ottawa.

TCD
6, 4517–4555, 2012

References

ACGR: Glossary of Permafrost and Related Ground-Ice Terms, National Research of Canada, Technical Memorandum No. 142, 64 pp., 1988.

Arctic Climate Impact Assessment, Cambridge: Cambridge University Press, available at: http://www.acia.uaf.edu, p. 1042, 2005.

Bonnaventure, P. P. and Lewkowicz, A. G.: Mountain permafrost probability mapping using the BTS method in two climatically dissimilar locations, northwest Canada, Can. J. Earth Sci., 45, 443–455, 2008.

Bonnaventure, P. P. and Lewkowicz, A. G.: Modelling climate change effects on the spatial distribution of mountain permafrost at three sites in northwest Canada, Climatic Change, 105, 293–312, doi:10.1007/s10584-010-9818-5, 2010.

Bonnaventure, P. P. and Lamoureux, S. F.: The active layer: a conceptual review of monitoring, modelling techniques and changes in a warming climate, Prog. Phys. Geog., submitted, 2012.

Bonnaventure, P. P. and Lewkowicz, A. G.: Permafrost probability modelling above and below treeline, Yukon, Canada, Cold Reg. Sci. Technol., 79–80, 92–106, doi:10.1016/j.coldregions.2012.03.004, 2012.

Burn, C. R.: Permafrost, tectonics, and past and future regional climate change, Yukon and adjacent Northwest Territories, Can. J. Earth Sci., 31, 182–191, 1994.

Burn, C. R. and Nelson, F. E.: Comment on "A projection of severe near-surface permafrost degradation during the 21st century" by David M. Lawrence and Andrew G. Slater, Geophys. Res. Lett., 33, L21503, doi:10.1029/2006GL027955, 2006.

Burn, C. R. and Zhang, Y.: Sensitivity of active-layer development to winter conditions north of treeline, Mackenzie delta area, western Arctic coast, 6th Canadian Permafrost Conference, Calgary, Canada, 2010.

CAS (Canadian Standards Association): Technical guide: Overview of key considerations relating to community infrastructure, permafrost and climate change, Canadian standards association, Mississauga, Ontario, Canada. 2010.

Clements, C. B., Whiteman, C. D., and Horel, J. D.: Cold-air pooling structure and evolution in a mountain basin: Peter Sinks, Utah, J. Appl. Meteorol., 42, 752–768, 2003

TCD
6, 4517–4555, 2012

Department of Energy Mines and Resources, Canada: Physiographic regions of Yukon and surrounding Canadian territory, Climate of Yukon, Canadian Government Publishing Centre, 1974.
Dorren, L. K. A.: A Review of Rockfall Mechanics and Modelling Approaches, Prog. Phys. Geog., 27, 69–87, 2003.
Duk-Rodkin, A.: Surficial geology, Dawson, Yukon Territory, Geol. Surv. Can., open file 3288, 1 : 250 000 scale, 1996.
Evans, S. G. and Clague, J. J.: Recent climatic change and catastrophic geomorphic processes in mountain environments, Geomorphology, 10, 107–128, 1994.
Eyles, N. and Miall, A.: Canada Rocks, The Geologic Journey, Fitzhenry and Whiteside limited, Markham Ontario, 2007.
Farnell, R., Hare, P. G., Blake, E., Bowyer, V., Schweger, C., Greer, S., and Gotthardt, R.: Multidisciplinary Investigations of Alpine Ice Patches in Southwest Yukon, Canada, Arctic, 57, 247–259, 2004.
French, H. M.: The Periglacial Environment third edition, John Wiley and Sons Inc., 111 River Street, Hoboken, NJ 07030, USA, 2007.
Froese, D. G., Westgate, J. A., Reyes, A. V., Enkin, R. J., and Preece, S. J.: Ancient permafrost and a future, warmer arctic, Science, 321, 5896, doi:10.1126/science.1157525, 2008.
Global Terrestrial Network for Permafrost (GTNP database): available at: http://www.gtnp.org/, 2011.
Gruber, S. and Hoelzle, M.: Statistical modeling of mountain permafrost distribution: Local calibration and incorporation of remotely sensed data, Permafrost Periglac., 12, 69–77, 2001.
Gruber, S. and Haeberli, W.: Mountain permafrost, in: Permafrost Soils, edited by: Margesin, R., available at: http://www.geo.unizh.ch/~stgruber/pubs/gruber_2009_pf-soils.pdf, Biology Series Vol. 16, Springer, 33–44, doi:10.1007/978-3-540-69371-0_3, 2009.
Haeberli, W., Guodong, C., Gorbunov, A. P., and Harris, S. A.: Mountain permafrost and climatic change, Permafrost Periglac., 4, 165–174, 1993.
Haeberli, W., Hallet, B., Arenson, L., Elconin, R., Humlum, O., Kaab, A., Kaufmann, V., Ladanyi, B., Matsuoka, N., Springman, S., and Vonder Mühll, D.: Permafrost Creep and Rock Glacier Dynamics, Permafrost Periglac., 17, 189–214, 2006.
Harris, C., Davies, M. C. R., and Etzelmüller, B.: The assessment of potential geotechnical hazards associated with mountain permafrost in a warming global climate, Permafrost Periglac., 12, 145–156, 2001.

TCD
6, 4517–4555, 2012

Heginbottom, J. R., Dubreuil, M. A., and Haker, P. T.: Canada Permafrost, (1 : 7 500 000 scale), in: The National Atlas of Canada, 5th Edn., sheet MCR 4177, Ottawa, National Resources Canada, 1995.
Hugelius, G., Kuhry, P., Tarnocai, C., and Virtanen, T.: Soil Organic Carbon Pools in a Periglacial Landscape: a Case Study from the Central Canadian Arctic, Permafrost Periglac., 21, 16–29, 2010
IPCC: available at: http://www.ipcc.ch/ipccreports/assessments-reports.htm, 2007.
Janke, J. R.: Modelling past and future alpine permafrost distribution in the Colorado front range, Earth Surf. Proc. Land., 30, 1495–1508, 2005.
Jorgenson, M. T., Racine, C. H., Walters, J. C., and Osterkamp, T. E.: Permafrost degradation and ecological changes associated with a warming climate in central Alaska, Climatic Change, 48, 551–579, 2001
Kääb, A.: Remote sensing of permafrost-related problems and hazards, Permafrost Periglac., 19, 107–136, 2008.
Kneisel, C., Rothenbuhler, C., Keller, F., and Haeberli, W.: Hazard assessment of potential periglacial debris flows based on GIS-based spatial modelling and geophysical field surveys: A case study in the Swiss Alps, Permafrost Periglac., 18, 259–268, 2007.
Kremer, M., Lewkowicz, A. G., Bonnaventure, P. P., and Sawada, M. C.: Utility of classification and regression tree analyses and vegetation in mountain permafrost models, Yukon Territory, Canada, Permafrost Periglac., 22, 163–178, 2011.
Lawrence, D. M., Slater, A. G., Romanovsky, V. E., and Nicolsky, D. J.: Sensitivity of a model projection of near-surface permafrost degradation to soil column and representation of soil organic matter, J. Geophys. Res., 113, F02011, doi:10.1029/2007JF000883, 2008.
Lewkowicz, A. G. and Ednie, M.: Probability mapping of mountain permafrost using the BTS method, Wolf Creek, Yukon Territory, Canada, Permafrost Periglac., 15, 67–80, 2004.
Lewkowicz, A. G. and Harris, C.: Frequency and Magnitude of active-layer detachment failures in discontinuous and continuous permafrost, northern Canada, Permafrost Periglac., 16, 115–130, 2005.
Lewkowicz, A. G. and Bonnaventure, P. P.: Interchangeability of Mountain Permafrost Probability Models, Northwest Canada, Permafrost Periglac., 19, 49–62, 2008.
Lewkowicz, A. G. and Bonnaventure, P. P.: Equivalent Elevation: a New Method to Incorporate Variable Lapse Rates Into Mountain Permafrost Modelling, Permafrost Periglac., 22, 153–162, 2011.

TCD
6, 4517–4555, 2012

Lewkowicz, A. G., Bonnaventure, P. P., Smith, S. L., and Kuntz, Z.: Spatial and thermal characteristics of mountain permafrost, Zorthwest Canada, Geogr. Ann., 94, 195–213, 2012.
Lipovsky, P. S., Coates, J., Lewkowicz, A. G., and Trochim, E.: Active-layer detachments following the summer 2004 forest fires near Dawson City, Yukon, in: Yukon Exploration and Geology 2005, edited by: Emond, D. S., Weston, L. H., Bradshaw, G. D., and Lewis, L. L., Yukon Geological Survey, 2006.
Natural Resources Canada: Forest ecosystems of Canada, available at: http://ecosys.cfl.scf.rncan.gc.ca/classification/classif08-eng.asp, 2010.
O'donnell, J. A., Harden, J. W., McGuire, A. D., and Romanovsky, V. E.: Exploring the sensitivity of soil carbon dynamics to climate change, fire disturbance and permafrost thaw in black spruce ecosystems, Biosciences, 8, 1367–1382, 2011.
Page, A.: M.Sc. Thesis, A topographic and photogrammetric study of rock glaciers in the southern Yukon Territory, 2009.
Pagès, M. and Miró, J. R.: Determining temperature lapse rates over mountain slopes using vertically weighted regression: a case study from the Pyrenees, Meteorol. Appl., 17, 53–63, 2009.
Romanovsky, V. E., Smith, S. L., and Christiansen, H. H.: Permafrost Thermal State in the Polar Northern Hemisphere during the International Polar Year 2007–2009: a Synthesis, Permafrost Periglac., 21, 106–116, 2010.
Shur, Y. and Jorgenson, M. T.: Patterns of Permafrost Formation and Degradation in Relation to Climate and Ecosystems, Permafrost Periglac., 18, 7–19, 2007.
Shur, Y., Hinkel, K. M., and Nelson, F. E.: The transient layer: Implications for geocryology and climate-change science, Permafrost Periglac., 16, 5–17, 2005.
Smith, S. L., Romanovsky, V. E., Lewkowicz, A. G., Burn, C. R., Allard, M., Clow, G. D., Yoshikawa, K., and Throop, J.: Thermal state of permafrost in North America – A contribution to the International Polar Year, Permafrost Periglac., 21, 117–135, 2010.
Snow, Water, Ice Permafrost in the Arctic (SWIPA): available at: www.amap.no/swipa, 2012.
Tarnocai, C., Canadell, J. G., Schuur, E. A. G., Kuhry, P., Mazhitova, G., and Zimov, S.: Soil organic carbon pools in the northern circumpolar permafrost region, Global Biogeochem. Cy., 23, GB2023, doi:10.1029/2008GB003327, 2009
Wahl, H. E., Fraser, D. B., Harvey, R .C., and Maxwell, J. B.: Climate of Yukon, Canadian Government Publishing Centre, 1987.

TCD
6, 4517–4555, 2012

Williams, P. J. and Smith, M. W.: The Frozen Earth: Fundamentals of Geocryology Cambridge University Press, The Edinbrugh Building, Shaftsbury Road, Cambridge CB2 2RU, 1989.
Woo, M. K., Kane, D. L., Carey, S. K., and Yang, D.: Progress in permafrost hydrology in the new millennium, Permafrost Periglac., 19, 237–254, 2008
Youngblut, D. K. and Luckman, B. H.: Maximum June–July temperatures in the southwest Yukon over the last 300 years reconstructed from tree-rings, Dendrochronologia, 25, 153–66, 2008.

TCD
6, 4517–4555, 2012

Table 1. Summary of different loss patterns according to region of area affected.

Loss type	Region affected	SLR range	Relation to elevation
SUSL	ESW	$-6.5\,\mathrm{K\,km^{-1}}$	Dependent.
CUSL	South & Mid	$<0\,\mathrm{K\,km^{-1}}$ but $>-6.5\,\mathrm{K\,km^{-1}}$	More dependent closer to $-6.5\,\mathrm{K\,km^{-1}}$ and approaching independent as $0\,\mathrm{K\,km^{-1}}$ is approached.
BSL	North	Positive ($>0\,\mathrm{K\,km^{-1}}$)	Close to independent.

TCD
6, 4517–4555, 2012

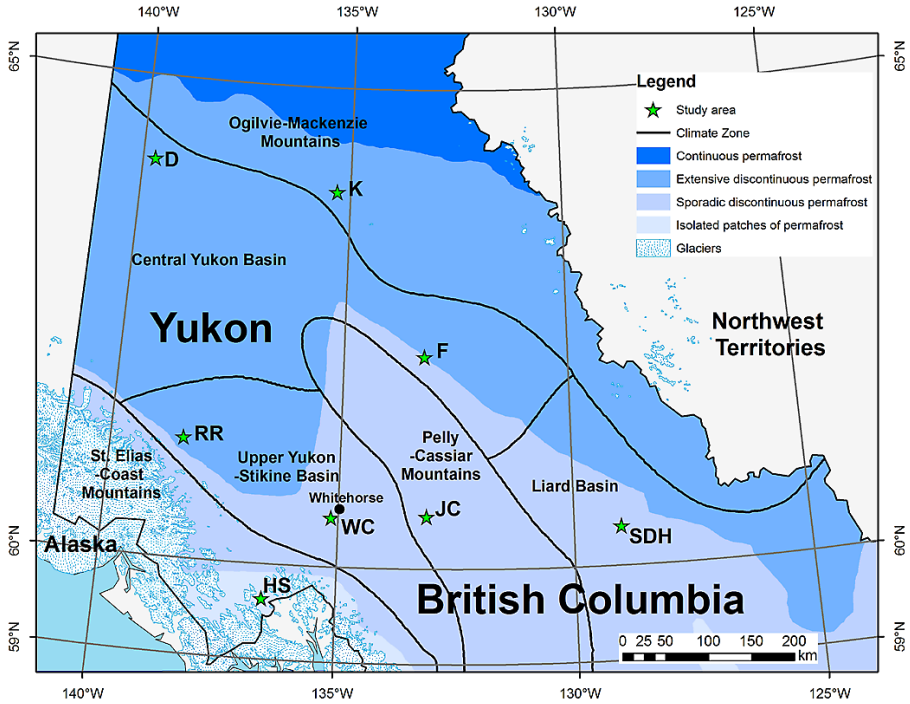

Fig. 1. Map of the study region showing modelling locations in relation to permafrost zones (Heginbottom et al. 1995) and climatic regions (Wahl et al., 1987). JC: Johnson's Crossing, SDH: Sa Dena Hes, F: Faro, K: Keno, D: Dawson, RR: Ruby Range, HS: Haines Summit and WC: Wolf Creek.

TCD
6, 4517–4555, 2012

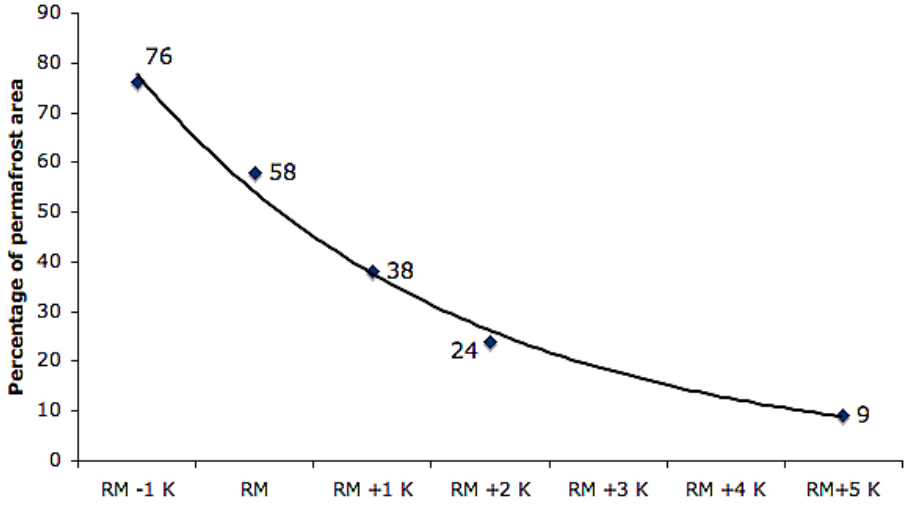

Fig. 2. Curve illustrating the pattern of permafrost distribution change according to climate modelling scenarios.

TCD
6, 4517–4555, 2012

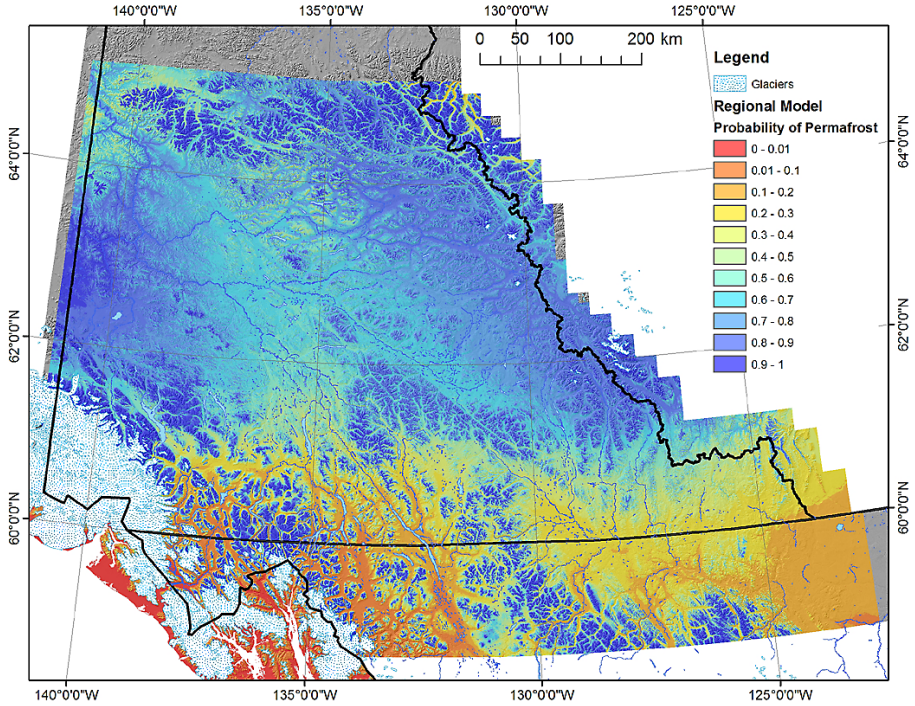

Fig. 3. Regional Model permafrost probability map, permafrost underlays 58 % of the unglaciated territory in this model (Bonnaventure et al., 2012).

TCD
6, 4517–4555, 2012

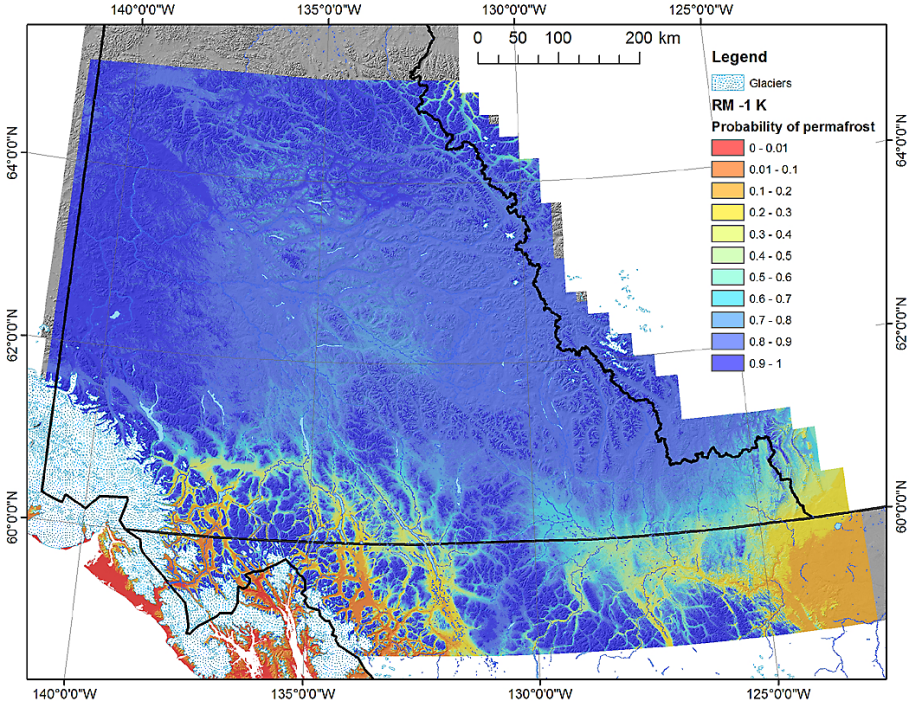

Fig. 4. Regional Model permafrost probability map with a −1 K climate change scenario applied to it, permafrost underlays 76 % of the region under this scenario.

TCD
6, 4517–4555, 2012

Scenario-based climate change modelling

P. P. Bonnaventure and A. G. Lewkowicz

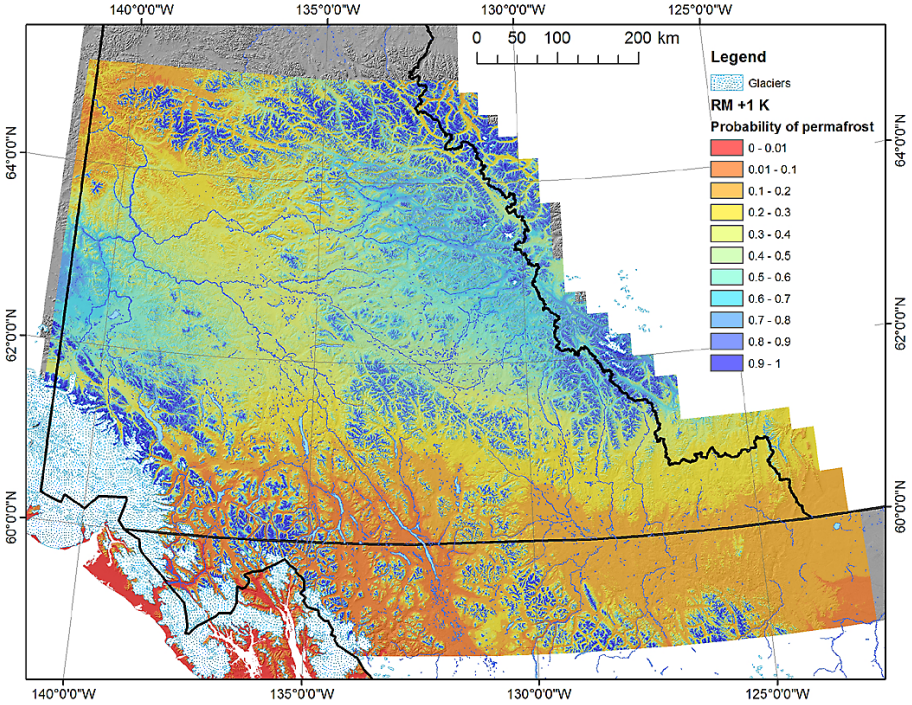

Fig. 5. Regional Model permafrost probability map with a +1 K climate change scenario applied to it, permafrost underlays 38 % of the region under this scenario.

TCD
6, 4517–4555, 2012

Scenario-based climate change modelling

P. P. Bonnaventure and A. G. Lewkowicz

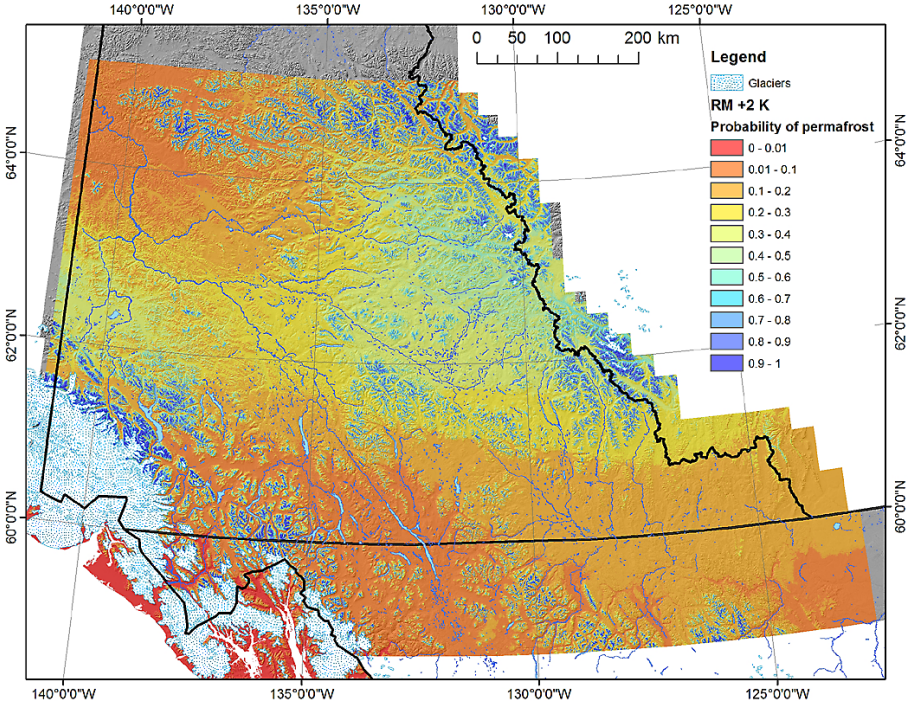

Fig. 6. Regional Model permafrost probability map with a +2 K climate change scenario applied to it, permafrost underlays 24 % of the region under this scenario.

TCD
6, 4517–4555, 2012

Scenario-based climate change modelling

P. P. Bonnaventure and A. G. Lewkowicz

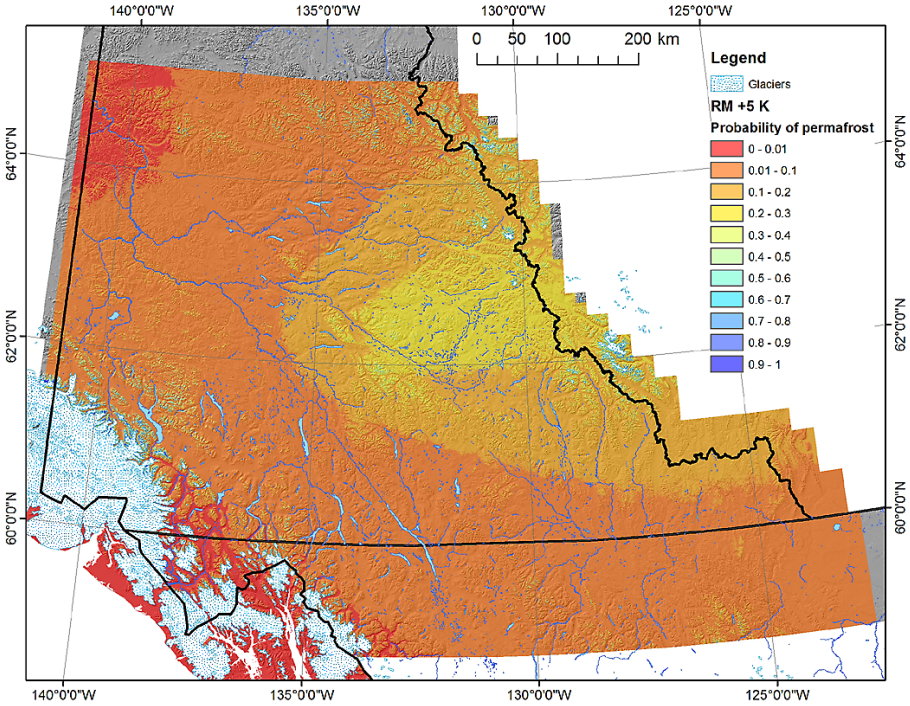

Fig. 7. Regional Model permafrost probability map with a +5 K climate change scenario applied to it, permafrost underlays 9 % of the region under this scenario.

TCD
6, 4517–4555, 2012

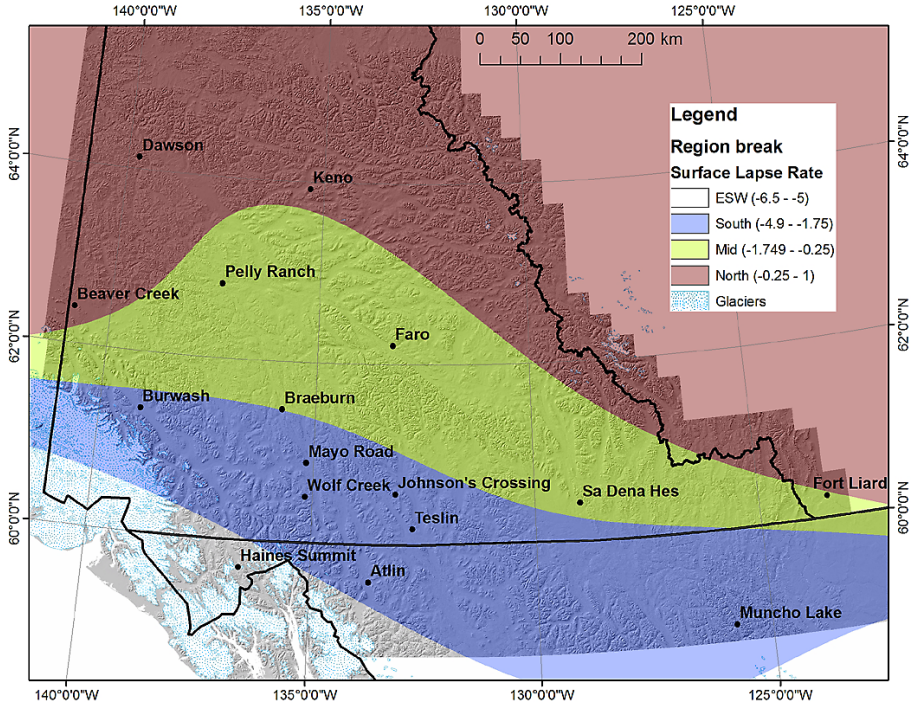

Fig. 8. Region break according to geographic area and common SLR.

TCD
6, 4517–4555, 2012

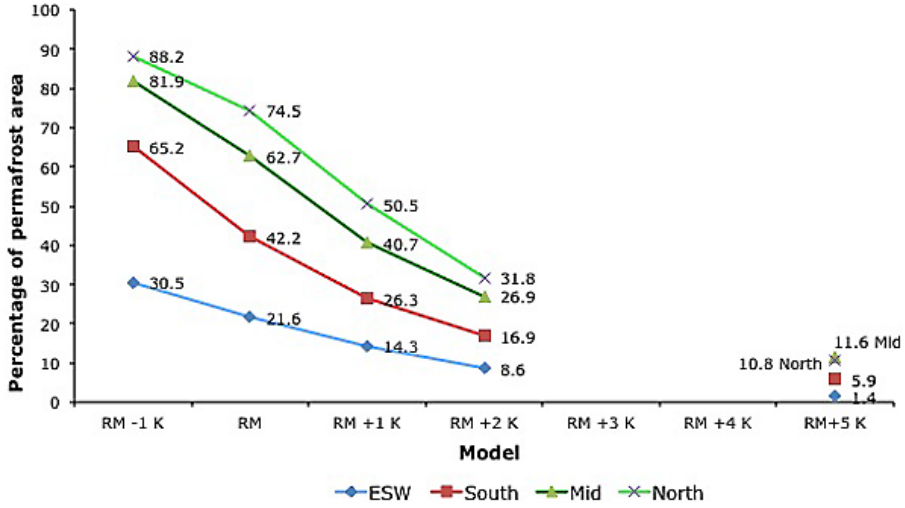

Fig. 9. Graph illustrating the pattern of overall permafrost loss through all MAAT scenarios for each of the zones in the region.

TCD
6, 4517–4555, 2012

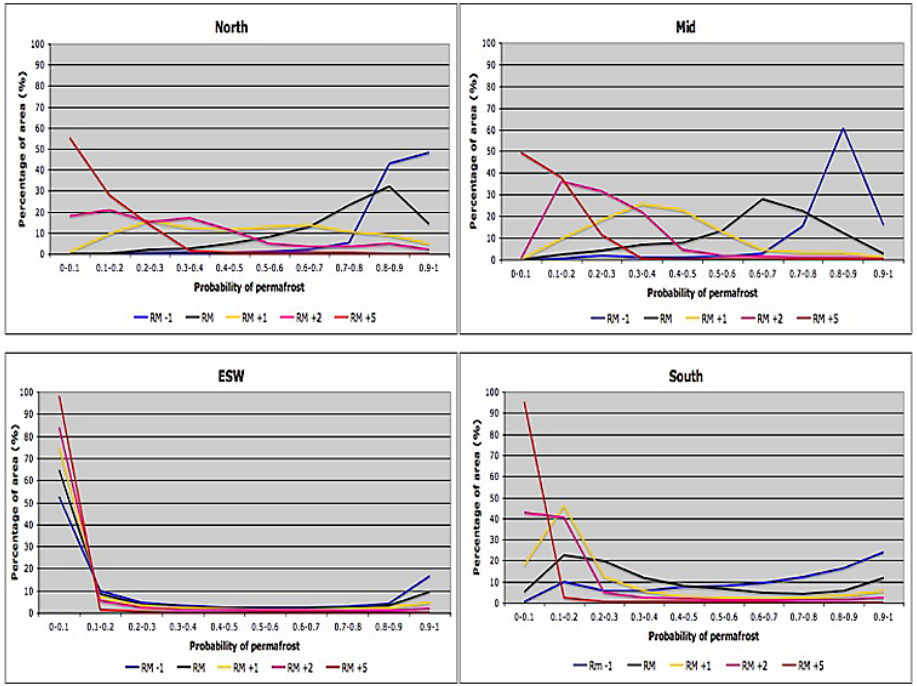

Fig. 10. Graphs illustrating the range of permafrost probabilities and the gain/loss pattern for specific regions for each climate change scenario including the base case. Permafrost probabilities are examined across 0.1 intervals in order to note the shift in the distribution peak.

TCD
6, 4517–4555, 2012

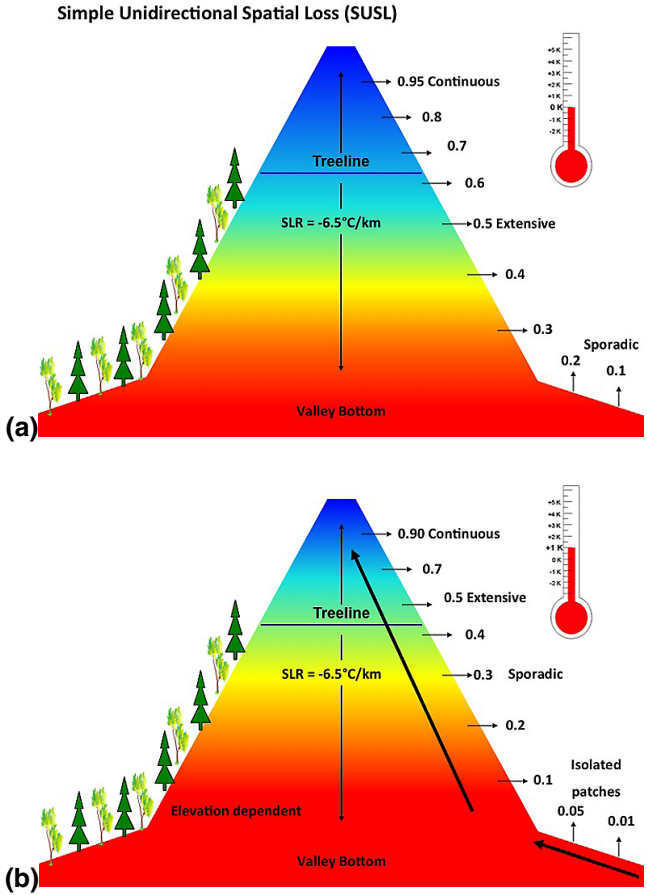

Fig. 11. (a) Typical permafrost probabilities in an area susceptible to Simple Unidirectional Spatial Loss before the incursion of a warming scenario and then following the warming scenario **(b)**.

TCD
6, 4517–4555, 2012

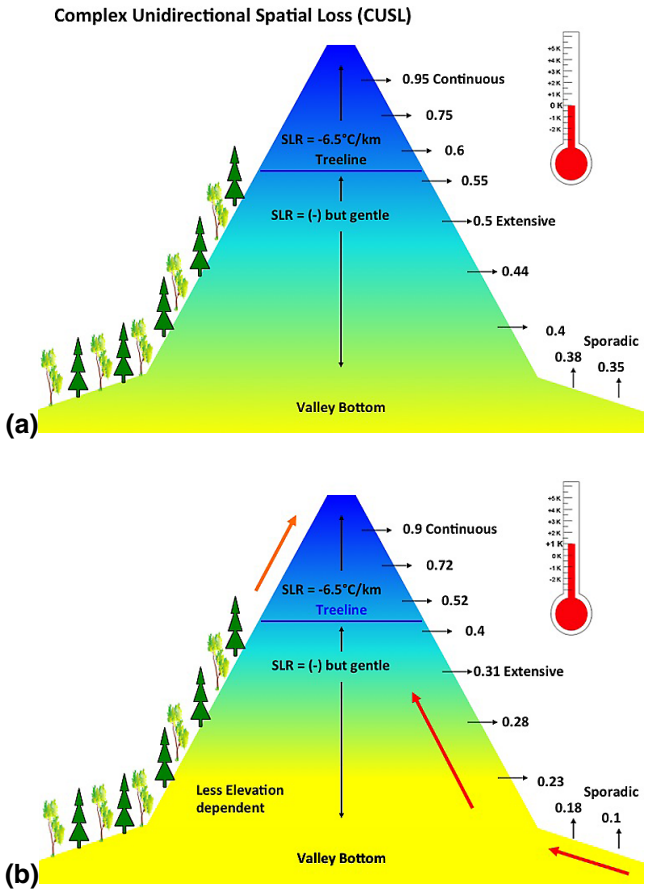

Fig. 12. (a) Typical permafrost probabilities in an area susceptible to Complex Unidirectional Spatial Loss before the incursion of a warming scenario and then following the warming scenario **(b)**.

TCD
6, 4517–4555, 2012

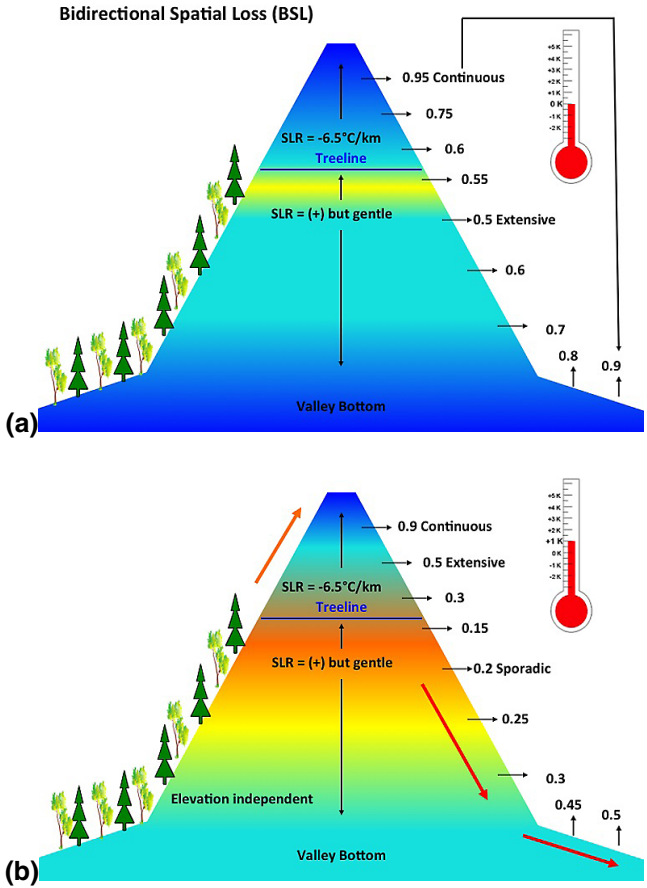

Fig. 13. (a) Typical permafrost probabilities in an area susceptible to Bidirectional Spatial Loss before the incursion of a warming scenario and then following the warming scenario **(b)**.

TCD
6, 4517–4555, 2012

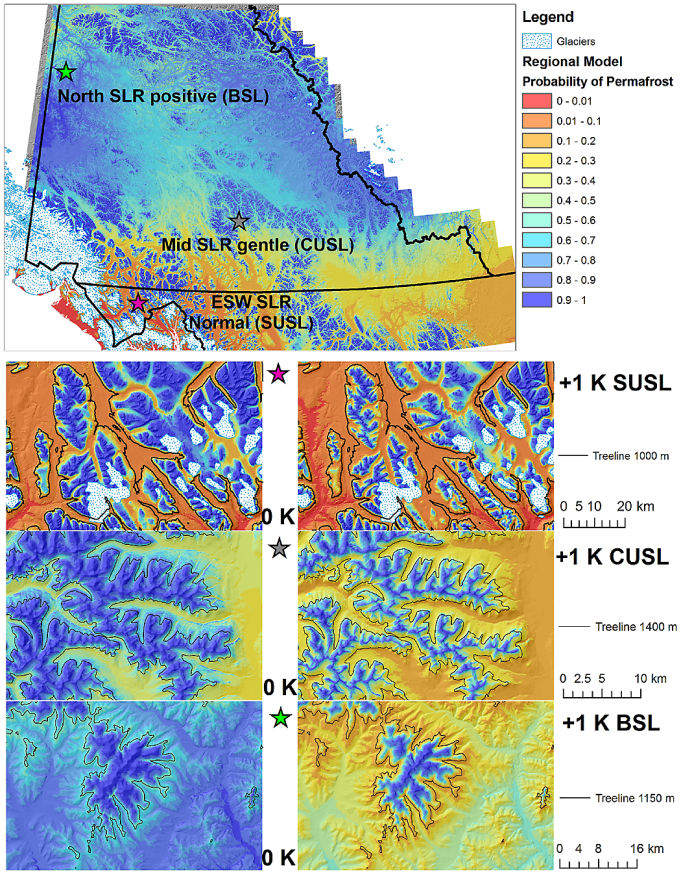

Fig. 14. Illustration of the different types of spatial loss from the Regional Model with a +1 K scenario applied according to different geographic locations for three distinct areas in the region.

TCD
6, 4517–4555, 2012

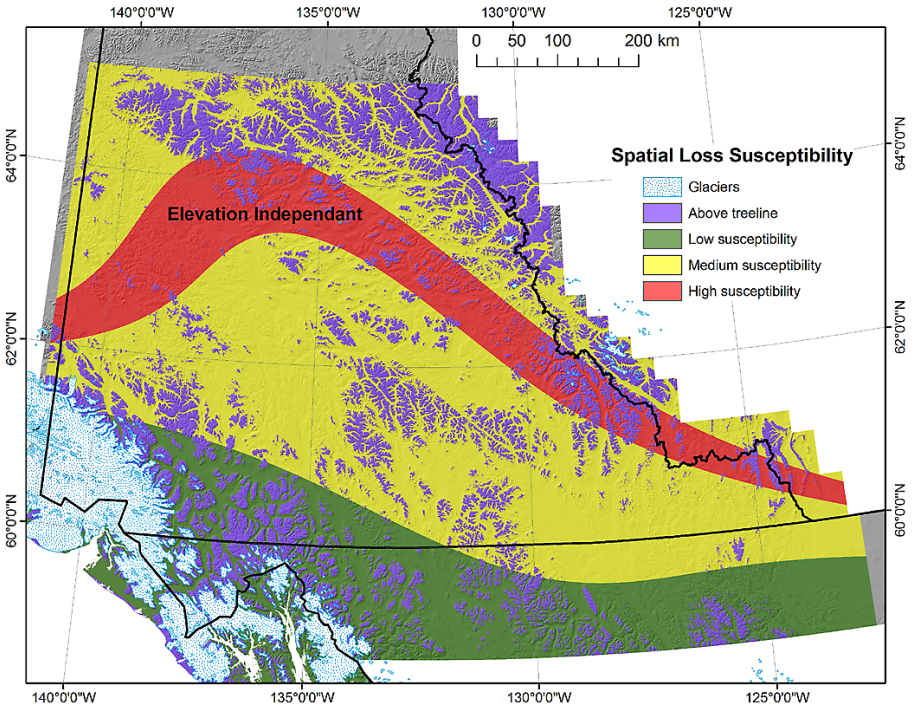

Fig. 15. Map of potential spatial loss susceptibility for the area of the Regional Model to short-term, small changes in MAAT (e.g. +1 K). Susceptibility is based on SLRs where areas with SLRs close to 0 K km^{-1} are said to be elevation independent meaning that when a given warming scenario is preformed all area within the zone is prone to permafrost loss.

TCD
6, 4517–4555, 2012